Published in European Journal of Inorganic Chemistry 2012, issue 4, 727-732, 2012
which should be used for any reference to this work

Superparamagnetic Core-Shell-Type Fe_3O_4/Ru Nanoparticles as Catalysts for the Selective Hydrogenation of an Unconstrained α,β-Unsaturated Ketone

Farooq-Ahmad Khan and Georg Süss-Fink*

Institut de Chimie, Université de Neuchâtel, Avenue de Bellevaux 51, 2000 Neuchâtel, Switzerland; Fax: +41-32-7182511
E-mail: georg.suess-fink@unine.ch

Dedicated to Dr. Christian Bruneau on the occasion of his 60th birthday

Keywords: Nanoparticles / Ruthenium / Hydrogenation / Supported catalysts

Superparamagnetic core-shell-type Fe_3O_4/Ru nanoparticles (particle size ca. 15 nm) synthesized by co-precipitation, adsorption and reduction methods were found to selectively hydrogenate the carbon-oxygen double bond in *trans*-4-phenyl-3-penten-2-one (conversion 100 %, selectivity > 90 %) with a catalytic turnover of 900 under mild reaction conditions (30 °C, 15 bar H_2). The finely dispersed catalyst can be separated from the reaction mixture by using an external magnet, recycled, and reused without significant loss of activity and selectivity.

Introduction

Selective hydrogenation of the carbon-oxygen bond in α,β-unsaturated carbonyl compounds is a synthetic challenge, since C=C bond reduction is thermodynamically more favorable (35 kJ mol^{-1}) than C=O bond reduction.[1] This problem becomes even more complicated by the presence of an aromatic substituent in such systems because of possible ring hydrogenation.[2] Moreover, the transformation of unsaturated ketones into unsaturated alcohols is more difficult than that of unsaturated aldehydes, because ketones are sterically more hindered.[3] In addition, the "promoter effect" to enhance selectivity is also absent in the case of unsaturated ketones.[4]

In a pioneering study, Szöllosi et al. evaluated the potential of different metals such as Pt, Pd, Rh, Ru, Cu, and Ni supported on silica for the selective hydrogenation of α,β-unsaturated ketones.[5] Later, von Arx et al. were able to attain >90% chemoselectivities for a sterically hindered C=O bond in ketoisophoron over alumina-supported Pt and Pd catalysts.[6] Such a remarkable selectivity might be attributed to steric effects,[1b,3] because the presence of bulky substituents at the olefin double bond presumably hampers its adsorption at catalytic sites.[8] Milone et al. and Mertens et al. showed that unsaturated alcohols can be obtained from different α,β-unsaturated ketones with a selectivity higher than 60% at a conversion of 90% by using a gold catalyst.[4,8] Recently, Wang et al. also used gold supported on mesostructured CeO_2 to hydrogenate *trans*-4-phenyl-3-penten-2-one at 100 °C with 63% selectivity for the unsaturated alcohol.[9] However, in spite of extensive studies, efforts to selectively hydrogenate α,β-unsaturated ketones to give the corresponding unsaturated alcohols by molecular hydrogen have not been very successful.[8a,9]

Thus, the synthesis of unsaturated alcohols is mainly achieved with hazardous metal hydrides such as $LiAlH_4$ and $NaBH_4$,[10] with silicon hydrides,[11] or by transfer hydrogenation,[8a,12] as well as by Meerwein–Ponndorf–Verley-type reduction methods.[13] Homogeneous transition-metal catalysts sometimes show high selectivity,[14] but such complexes are often inefficient or have limited reusability.[15] Moreover, the separation of these complexes from the reaction mixture is very difficult.[16] Thus, the development of a highly selective, easily recoverable, and recyclable heterogeneous catalyst for the hydrogenation of unsaturated ketones remains a demanding task,[1a] because unsaturated alcohols are important intermediates used in the production of fine chemicals, pharmaceuticals, perfumery, and food processing industries.[17]

In chemical technology, heterogeneous catalysts are usually preferred, because separation, recovery, and recycling of the catalyst are relatively easy.[18] However, in liquid-phase batch reactions, the separation of the catalyst from the reaction products is still problematic.[19] Therefore, environmentally friendly, cost-effective, robust, easily recoverable, and cleanly reusable catalysts would be highly desirable[16] to ensure minimum loss, enhance their lifetime and minimize the consumption of auxiliary substances used in achieving separations.[19]

Recently, the use of magnetic materials as catalyst supports has attracted much attention,[16] because solid catalysts with magnetic properties can efficiently be separated

from the reaction mixture by applying an external magnetic field.[20] This green and sustainable approach has many advantages over traditional time- and solvent-consuming processes, since it provides a fast, economical, and environmentally acceptable way to separate products and recycle catalysts.[19] Thus, ferromagnetic iron–nickel nanoparticles encapsulated in carbon have been prepared by Teunissen et al.; the carbon coating is necessary to overcome the problem of clustering of the nanoparticles.[21]

Superparamagnetic nanoparticles are such materials with high surface area,[22] which can be easily dispersed in solution, because they are intrinsically non-magnetic and therefore show no tendency to aggregate in solution.[18] On the other hand, these nanoparticles can be recovered easily from the reaction mixture by applying an external magnetic field, thus offering better handling properties.[19]

In this paper, we report on superparamagnetic core-shell-type Fe_3O_4/Ru nanoparticles, synthesized by immobilisation of $[(C_6H_6)Ru(H_2O)_3]^{2+}$ cations on freshly prepared magnetite nanoparticles, followed by reduction with molecular hydrogen. They are highly active and selective in the catalytic conversion of *trans*-4-phenyl-3-penten-2-one into 4-phenylbutan-2-ol.

Results and Discussion

Nanosized magnetite (Fe_3O_4) was prepared by the co-precipitation method,[23] by adding an aqueous solution of a 1:2 mixture of $FeCl_2$ and $FeCl_3$ to ammonia (0.7 M), followed by vigorous stirring. The black Fe_3O_4 nanoparticles thus obtained are sensitive to air and must be handled in an inert atmosphere.[24] The NH_4^+ cations adsorbed at the surface of these particles are partially exchanged by Na^+ by adjusting the pH to 10 by using NaOH (2 M).[23b] The Fe_3O_4 nanoparticles containing Na^+ and NH_4^+ at their surface are isolated from the solution by magnetic decantation and further used without washing with water.

$$Fe^{2+}_{(aq)} + 2\,Fe^{3+}_{(aq)} + 8\,OH^-_{(aq)} \longrightarrow Fe_3O_{4(s)} + 4\,H_2O_{(l)}$$

The dinuclear complex, the benzene ruthenium dichloride dimer, dissolves in water with hydrolysis to give, with successive substitution of the chlorido ligands by aqua ligands, a mixture of mononuclear benzene ruthenium complexes in equilibrium.[25] The benzene ^1H NMR signals of the D_2O solution are assigned to $[(C_6H_6)RuCl_2(H_2O)]$ (δ = 5.89 ppm), $[(C_6H_6)RuCl(H_2O)_2]^{2+}$ (δ = 5.97 ppm), and $[(C_6H_6)Ru(H_2O)_3]^{2+}$ (δ = 6.06 ppm).[26] The dication $[(C_6H_6)Ru\,(H_2O)_3]^{2+}$, which was isolated as the sulfate and structurally characterized,[27] is the major species present in the hydrolytic mixture over the pH range 5–8 according to the NMR spectrum.

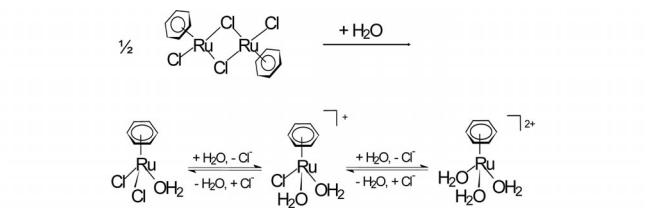

When the yellow solution obtained by dissolving the dinuclear complex $[(C_6H_6)RuCl_2]_2$ in water is added to the magnetite nanoparticles described above, the main hydrolysis product, $[(C_6H_6)Ru(H_2O)_3]^{2+}$, adsorbs on the surface of the nanosized Fe_3O_4 (replacing the appropriate amount of counterions) to give the ruthenium(II)-modified magnetite **1**. This material is isolated by magnetic decantation, washed with deoxygenated water, and dried under vacuum. Inductively coupled plasma optical emission spectroscopy (ICP–OES) analysis of this material shows a ruthenium loading of 0.074 mmol per gram of Fe_3O_4, which is the maximum loading. The Fourier transform infrared (FTIR) spectrum indicates the presence of an absorption band at 576 cm^{-1}, which can be assigned to Fe–O vibrations of bulk Fe_3O_4.[28] Ruthenium(II)-modified magnetite **1** reacts with hydrogen under pressure (50 bar) at 100 °C in *n*BuOH by reduction of the adsorbed $[(C_6H_6)Ru(H_2O)_3]^{2+}$ species to metallic ruthenium to give core-shell-type Fe_3O_4/Ru nanoparticles **2** (Scheme 1), in a manner similar to that for the preparation of hectorite-supported ruthenium nanoparticles.[29]

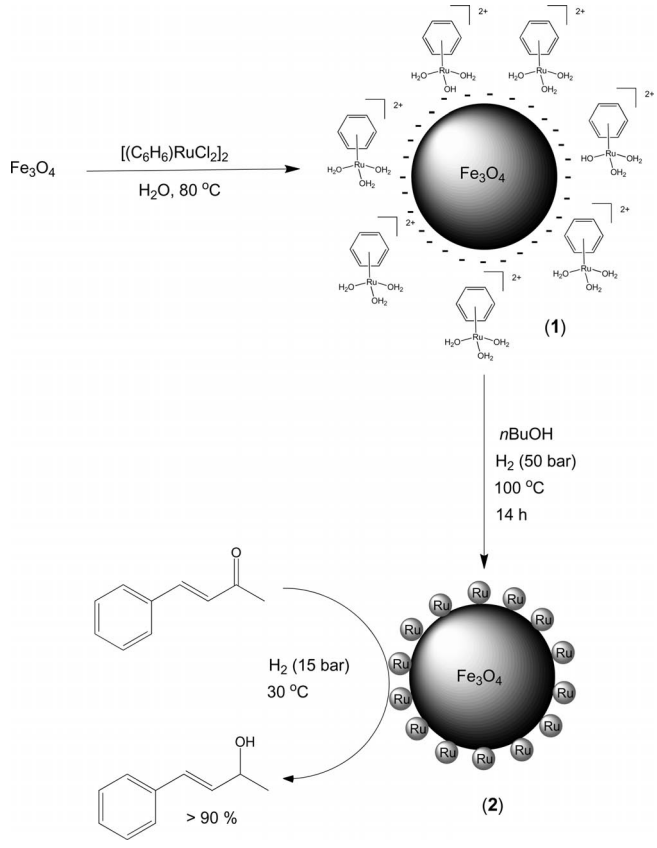

Scheme 1. Synthesis of superparamagnetic core–shell-type Fe_3O_4/Ru nanoparticles and their catalytic action.

Figure 1 shows the TEM micrograph of **2** before the catalytic reaction. The size distribution of these superparamagnetic Fe_3O_4/Ru nanoparticles was studied by transmission electron microscopy (TEM) by using the "ImageJ" software[30] for image processing and analysis. The mean particle size was calculated by using the equation: $\bar{d} = \Sigma n_i d_i / n_i$.[4]

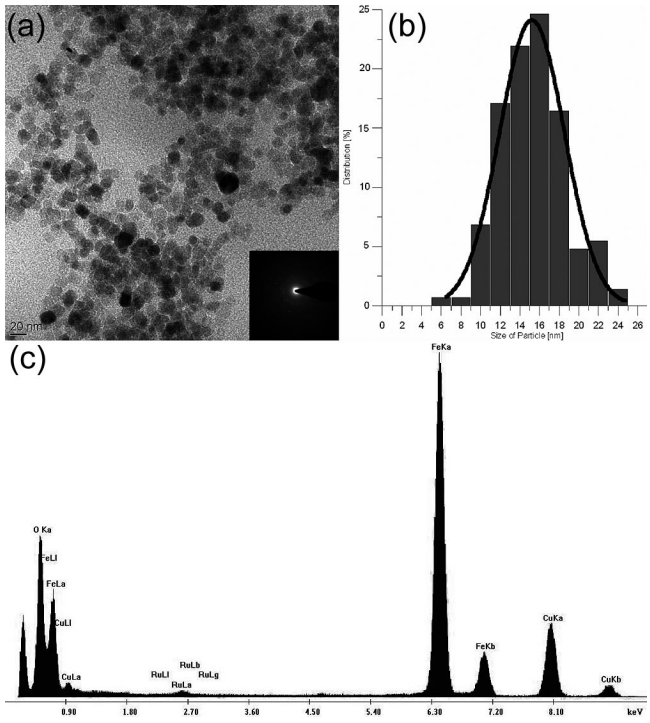

Figure 1. (a) TEM micrograph with SAED, (b) histogram (the bars show the size distributtion and the solid line the Gaussian fit), and (c) EDAX analysis of core-shell-type Fe_3O_4/Ru nanoparticles **2**.

Some aggregation of the nanoparticles was observed, presumably because *n*BuOH is not very effective in preventing the aggregation of these particles. However, *n*BuOH favors the accessibility of the substrate to catalytically active sites on the nanoparticles.[31] The micrographs show particles varying from 5 to 25 nm, the average particle size is 15 nm, which is close to the boundary between superparamagnetic and single domains. The mean particle size and standard deviation (σ) were estimated from image analysis of about at least 100 particles. The presence of ruthenium was inferred from energy dispersive X-ray spectroscopic (EDAX) analysis, which was further confirmed by inductively coupled plasma optical emission spectroscopy (ICP-OES). The percent weight loss of **2** as a function of temperature was studied by thermogravimetric analysis (TGA), which shows an overall weight loss of ca. 3% between 180–445 °C. This loss may be attributed to the loss of *n*BuOH molecules adsorbed at the surface of **2**.

The X-ray powder diffraction of Ru^0-modified magnetite **2** nanoparticles is shown in Figure 2. The average crystallite size of 14.4 nm was estimated by applying the Scherrer formula[32] on the full widths at half maximum (0.89) of the strongest (100%) reflection; the value of 2θ is 35.59°.

Figure 3 shows the magnetization curves for ruthenium-(II)-modified magnetite nanoparticles **1** and Ru^0-modified magnetite **2** nanoparticles measured at room temperature. These modified nanoparticles have a saturation magnetization (σ_s) of 62.4 and 69.6 emu/g, respectively. These values are slightly smaller than that of bulk magnetite (92 emu/g),

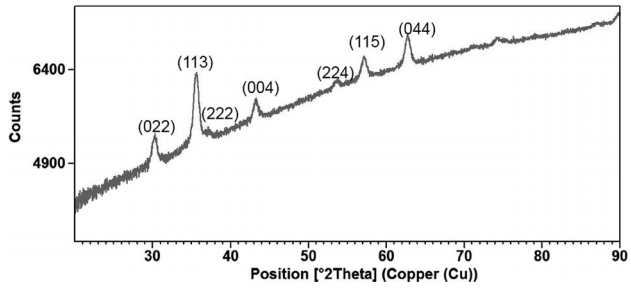

Figure 2. X-ray powder diffraction of the Ru^0-modified magnetite **2**.

which is consistent with the presence of surface coatings with ruthenium.[22] At low magnetic field, the hysteresis loops of these nanoparticles (insets in Figure 3) indicate low coercivity and almost zero remanence, which suggests that the particles exhibit superparamagnetic behavior. The slightly opened loop can be attributed to particles with grain size larger than ca. 20 nm that still can carry remanent magnetization during the measurement duration of 100 ms.

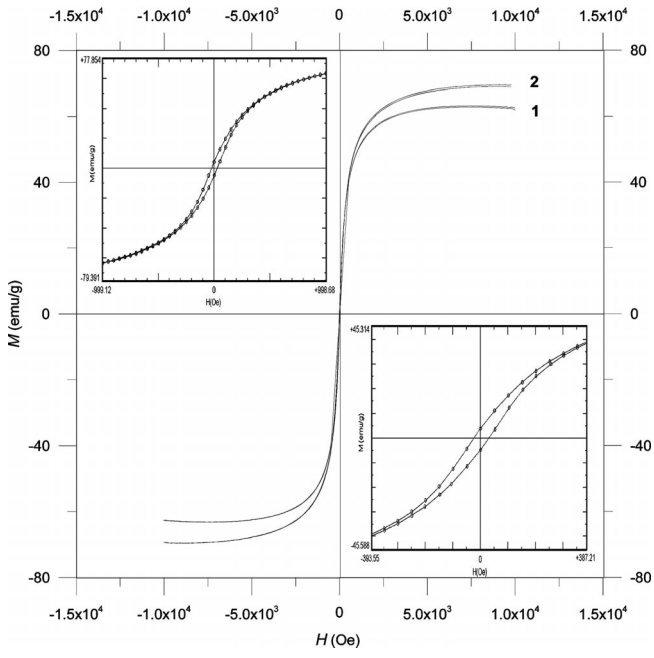

Figure 3. Magnetization curves for **1** and **2** measured at 300 K. The insets show magnified hysteresis loops at low magnetic fields, which highlight the coercivity and remanence of the particles. These particles exhibit predominantly superparamagnetic behavior with some blocked, single-domain particles.

The core-shell-type Fe_3O_4/Ru nanoparticles **2**, which are intrinsically nonmagnetic can be readily dispersed in *n*BuOH and easily recovered by applying an external magnetic field (Figure 4). They are a highly active and selective hydrogenation catalyst, which convert *trans*-4-phenyl-3-penten-2-one under hydrogen into 4-phenylbutan-2-ol and avoid the formation of saturated products (Scheme 2).

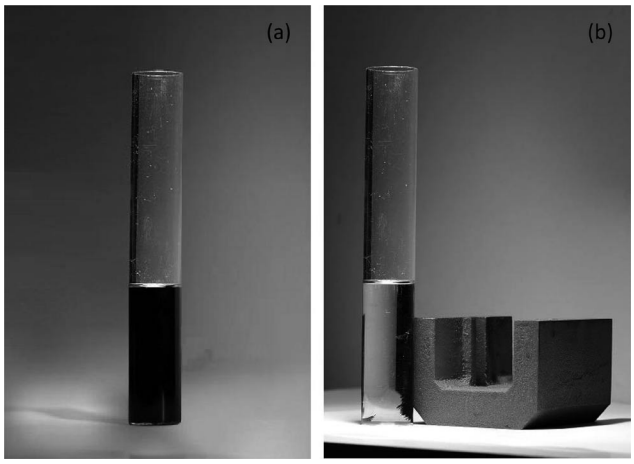

Figure 4. Superparamagnetic core-shell-type Fe_3O_4/Ru nanoparticles (a) dispersed in *n*BuOH and (b) gathered on the glass wall by an external magnet.

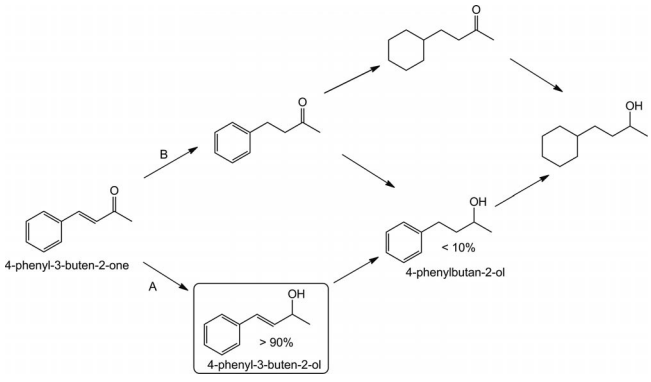

Scheme 2. Selective hydrogenation of *trans*-4-phenyl-3-buten-2-one and possible reaction pathway.

This highly selective reduction of an unconstrained α,β-unsaturated ketone is striking, especially, since no aromatic ring hydrogenation was observed. Thus, the catalyst is capable of reducing the C=O bond selectively. The catalytic reaction was followed by a gas chromatography coupled to mass spectrometry detector (GC–MS). The products were separated on an apolar column and were identified by their retention time and mass spectrum by using the electron impact (EI) ionization method.

The hydrogenation of *trans*-4-phenyl-3-penten-2-one was carried out by using **2** freshly prepared by the reduction of **1** in *n*BuOH (20 mL) under a pressure of hydrogen (50 bar) at 100 °C for 14 h. GC–MS shows complete conversion of the substrate (100%). The overall selectivity of **2** towards unsaturated alcohols was >90%, presumably because of the mild reaction conditions and the interaction between the catalyst and the support. The turnover number was determined by adding 12.2 mmol (1.78 g) of *trans*-4-phenyl-3-penten-2-one after regular intervals, until the catalyst became almost inactive; the total mass of substrate added was 5.34 g. Table 1 shows the time dependence of the catalytic hydrogenation, which is linear before saturation (Figure 5).

Table 1. Hydrogenation of *trans*-4-phenyl-3-penten-2-one with Fe_3O_4/Ru nanoparticles in *n*-butanol.

Time (h)	Substrate conversion (%)	Unsaturated alcohol (%)	Unsaturated alcohol selectivity (%)
1	15.2	14.3	94.1
2	32.4	30.9	95.4
3	49.3	46.8	94.9
4	69.0	63.1	91.5
5	88.0	79.5	90.3
6	98.8	89.7	90.8
7	100	92.8	92.8

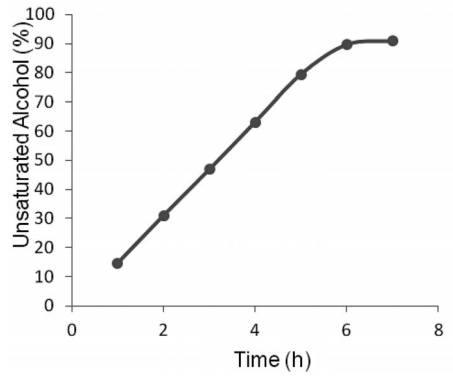

Figure 5. Time dependence of the hydrogenation of *trans*-4-phenyl-3-penten-2-one catalyzed by Ru^0-coated magnetite **2**.

A schematic representation of the reaction pathway (Scheme 2) shows that the reaction undergoes path A and not path B, because no traces of 4-phenylbutan-2-one were observed during GC–MS analysis of the reaction mixtures taken at different reaction times. It may be assumed that the saturated alcohol 4-phenylbutan-2-ol is essentially obtained by further reduction of the unsaturated alcohol 4-phenyl-3-buten-2-ol. Interestingly, no traces of 4-cyclohexylbutan-2-one and 4-cyclohexylbutan-2-ol were observed, which suggests that **2** is unable to catalyze aromatic ring hydrogenation under the reaction conditions.

The high selectivity for hydrogenation of the C=O bond can tentatively be attributed to the activation of the C=O bond by the metal–support interaction. It can be assumed that magnetite probably modifies the electronic properties of ruthenium, which in turn, leads to an increase in the hydrogenation selectivity for the C=O bond. Thus, the specific hydrogenation tendency of *trans*-4-phenyl-3-penten-2-one can be interpreted in terms of an exclusive adsorption of C=O bonds at the surface of the nanoparticles.[7a]

The nanoparticles **2** can be recovered and reused, however, after three catalytic runs, aggregation was observed (Figure 6). In order to determine the amount of ruthenium leaching, the combined washings of three consecutive runs are analyzed by ICP-OES. As there was no iron peak in the spectrum, which could interfere with the ruthenium signals, the ruthenium quantity could be calculated without applying any correction. The leaching observed is around 4.1% with respect to original ruthenium loading after three catalytic runs.

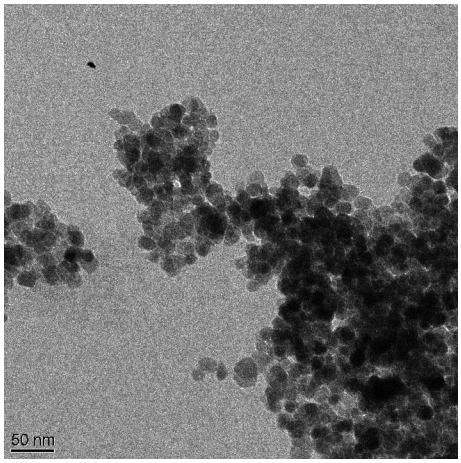

Figure 6. TEM micrograph of **2** after three catalytic runs.

Conclusions

We have prepared novel core-shell-type Fe_3O_4/Ru nanoparticles, which show a remarkable catalytic activity for the selective hydrogenation of the C=O bond in an unconstrained α,β-unsaturated ketone viz. *trans*-4-phenyl-3-penten-2-one. These environmentally friendly superparamagnetic nanoparticles can be easily dispersed because of the intrinsically nonmagnetic nature and can be readily recycled and reused by magnetic decantation.

Experimental Section

Preparation of Fe_3O_4 Nanoparticles: Fe_3O_4 nanoparticles were prepared by the co-precipitation method:[23] A freshly prepared aqueous solution of 1 M $FeCl_3$ was mixed with 2 M $FeCl_2$ (2.5 mL) dissolved in 2 M HCl. Both solutions were prepared in deoxygenated water. Immediately after the solutions were mixed under nitrogen, it was added to NH_3 (125 mL of a 0.7 M solution) under N_2. After 30 min of vigorous stirring, the pH was adjusted to 10 by using a 2 M NaOH. After 1 h, the black Fe_3O_4 nanoparticles formed were separated magnetically.

Preparation of Fe_3O_4/$[(C_6H_6)Ru(H_2O)_3]^{2+}$ (1): Fe_3O_4 nanoparticles were redispersed in water (50 mL) containing $[(C_6H_6)_2Ru_2Cl_4]$ (0.1 g). This mixture was heated at 80 °C overnight. The resulting precipitate was separated magnetically, washed with H_2O (3× 25 mL), and dried in vacuo.

Preparation of Fe_3O_4/Ru (2): 2 was obtained by reacting a suspension of **1** (0.5 g) in *n*BuOH (20 mL) in a magnetically stirred stainless-steel autoclave (volume 100 mL) under a pressure of H_2 (50 bar) at 100 °C for 14 h. After releasing the pressure and cooling, **2** was isolated by magnetic decantation and dried in vacuo.

Hydrogenation of *trans*-4-Phenyl-3-buten-2-one: Freshly prepared **2** (0.5 g) was added to a solution of *trans*-4-phenyl-3-buten-2-one (1.78 g) in *n*BuOH (20 mL). This solution was placed in an autoclave (100 mL), while being rigorously stirred at 30 °C under H_2 (15 bar). After every hour, the pressure was released, the sample was taken, and the solution was magnetically decanted from the solid and analyzed. The turnover number was determined by adding 1.78 g of substrate dissolved in *n*BuOH (20 mL) at regular intervals, until the catalyst became inactive; the total volume of substrate added was 5.34 g. The selectivity was checked by GC–MS. For recycling, a permanent magnet was externally applied to isolate **2** on the side wall of reactor. The reaction solution was decanted off, and the catalyst was reused directly for the next run.

Acknowledgments

Financial support of this work from the Fonds National Suisse de la Recherche Scientifique is gratefully acknowledged. We also thank the Johnson Matthey Research Centre for a generous loan of ruthenium(III) chloride hydrate. We are grateful to Professors Ann M. Hirt and Hans-Peter Hächler, Institute of Geophysics, ETH Zurich for magnetic measurements.

[1] a) P. Mäki-Arvela, J. Hájek, T. Salmi, D. Yu. Murzin, *Appl. Catal. A* **2005**, *292*, 1–49; b) S. N. Coman, V. I. Parvulescu, M. De Bruyn, D. E. De Vos, P. Jacobs, *J. Catal.* **2002**, 206–218.
[2] E. Breitner, E. Roginski, P. N. Rylander, *J. Org. Chem.* **1959**, *24*, 1855–1857.
[3] P. Kluson, L. Cerveny, *Appl. Catal. A* **1995**, *128*, 13–31.
[4] C. Milone, R. Ingoglia, A. Pistone, G. Neri, F. Frusteri, S. Galvagno, *J. Catal.* **2004**, *222*, 348–356.
[5] G. Szöllósi, Á. Mastalir, Á. Molnár, M. Bartók, *React. Kinet. Catal. Lett.* **1996**, *57*, 29–36.
[6] M. von Arx, T. Mallat, A. Baiker, *J. Mol. Catal. A* **1999**, *148*, 275–283.
[7] a) F. Delbecq, P. Sautet, *J. Catal.* **1995**, *152*, 217–236; b) F. Delbecq, P. Sautet, *Surf. Sci.* **1993**, *295*, 33–33; c) P. Sautet, J. F. Paul, *Catal. Lett.* **1991**, *9*, 245–260.
[8] a) C. Milone, R. Ingoglia, M. L. Tropeano, G. Neri, S. Galvagno, *Chem. Commun.* **2003**, 868–869; b) C. Milone, R. Ingoglia, L. Schipilliti, C. Crisafulli, G. Neri, S. Galvagno, *J. Catal.* **2005**, *236*, 80–90; c) P. G. N. Mertens, J. Wahlen, X. Ye, H. Poelman, D. E. De Vos, *Catal. Lett.* **2007**, *117*, 15–21; d) C. Milone, R. Ingoglia, S. Galvagno, *Gold Bull.* **2006**, *39*, 54–64.
[9] M.-M. Wang, L. He, Y.-M. Liu, Y. Cao, H.-Y. He, K.-N. Fan, *Green Chem.* **2011**, *13*, 602–607.
[10] a) A. M. Al-Etaibi, N. A. Al-Awadi, M. R. Ibrahim, Y. A. Ibrahim, *Molecules* **2010**, *15*, 407–419; b) N. M. Yoon, T. B. Sim, *Bull. Korean Chem. Soc.* **1993**, *14*, 749–752; c) A. L. Gemal, J. L. Luche, *J. Am. Chem. Soc.* **1981**, *103*, 5454–5459; d) K. E. Wilson, R. T. Seider, S. Masamune, *J. Chem. Soc. C* **1970**, 213; e) L. Mordenti, J. J. Brunet, P. Caubere, *J. Org. Chem.* **1979**, *44*, 2203–2205.
[11] a) H. Ozasa, K. Kondo, T. Aoyama, *Chem. Pharm. Bull.* **2010**, *58*, 989–990; b) T. Inagaki, Y. Yamada, L. T. Phong, A. Furuta, J. Ito, H. Nishiyama, *Synlett* **2009**, 253–256; c) D. Addis, S. Zhou, S. Das, K. Junge, H. Kosslick, J. Harloff, H. Lund, A. Schulz, M. Beller, *Chem. Asian J.* **2010**, *5*, 2341–2345; d) D. Addis, N. Shaikh, S. Zhou, S. Das, K. Junge, M. Beller, *Chem. Asian J.* **2010**, *5*, 1687–1691.
[12] a) N. Erathodiyil, S. Ooi, A. M. Seayad, Y. Han, S. S. Lee, J. Y. Ying, *Chem. Eur. J.* **2008**, *14*, 3118–3125; b) A. J. Blacker, S. M. Brown, C. Bubert, J. M. J. Williams, WO 0244111, **2002**; c) A. J. Blacker, B. V. Mellor, US patent 2002/0156282, **2002**.
[13] a) Y. Ishii, T. Nakano, A. Inada, Y. Kishigami, K. Sakurai, M. Ogawa, *J. Org. Chem.* **1986**, *51*, 240–242; b) M. Gargano, V. D′Orazio, N. Ravasio, M. Rossi, *J. Mol. Catal.* **1990**, *58*, L5; c) J. I. Di Cosimo, A. Acosta, C. R. Apesteguia, *J. Mol. Catal. A* **2004**, *222*, 87–96.
[14] a) K. Junge, B. Wendt, D. Addis, S. Zhou, S. Das, S. Fleischer, M. Beller, *Chem. Eur. J.* **2011**, *17*, 101–105; b) X. Chen, W. Jia, R. Guo, T. W. Graham, M. A. Gullons, K. Abdur-Rashid, *Dalton Trans.* **2009**, 1407–1410; c) I. Warad, Z. Al-Othman, S. Al-Resayes, S. S. Al-Deyab, E.-R. Kenawy, *Molecules* **2010**, *15*, 1028–1040; d) R. Noyori, T. Ohkuma, *Pure Appl. Chem.* **1999**,

71, 1493–1501; e) C. A. Mebi, R. P. Nair, B. J. Frost, *Organometallics* **2007**, *26*, 429–438.
[15] R. A. Sheldon, *Pure Appl. Chem.* **2000**, *72*, 1233–1246.
[16] V. Polshettiwar, R. Luque, A. Fihri, H. Zhu, M. Bouhrara, J.-M. Basset, *Chem. Rev.* **2011**, *111*, 3036–3075.
[17] a) J. Špringerova, P. Kacher, L. Červeny, *Res. Chem. Intermed.* **2005**, *31*, 785–795; b) B. S. Furniss, A. J. Hannaford, P. W. G. Smith, A. R. Tatchell in *Vogel's Textbook of Practical Organic Chemistry* (Ed.: A. Longman), 5th ed., Wiley-VCH, New York, **1989**, pp. 519.
[18] B. Panella, A. Vargas, A. Baiker, *J. Catal.* **2009**, *261*, 88–93.
[19] M. J. Jacinto, P. K. Kiyohara, S. H. Masunaga, R. F. Jardim, L. M. Rossi, *Appl. Catal. A* **2008**, *338*, 52–57.
[20] A. H. Lu, E. L. Salabas, F. Schuth, *Angew. Chem.* **2007**, *119*, 1242; *Angew. Chem. Int. Ed.* **2007**, *46*, 1222–1244.
[21] W. Teunissen, A. A. Bol, J. W. Geus, *Catal. Today* **1999**, *48*, 329–336.
[22] A. Hu, G. T. Yee, W. Lin, *J. Am. Chem. Soc.* **2005**, *127*, 12486–12487.
[23] a) L. M. Rossi, L. L. R. Vono, F. P. Silva, P. K. Kiyohara, E. L. Duarte, J. R. Matos, *Appl. Catal. A* **2007**, *330*, 139–144; b) R. Massart, *IEEE Trans. Magn.* **1981**, *17*, 1247–1248.
[24] W. Wu, Q. He, C. Jiang, *Nanoscale Res. Lett.* **2008**, *3*, 397–415.
[25] A. Meister, G. Süss-Fink, unpublished, see A. Meister, Ph. D. Thesis, University of Neuchâtel, Switzerland, **1994**.
[26] G. Meister, G. Süss-Fink, unpublished, see G. Meister, *Ph. D. Thesis*, University of Neuchâtel, Switzerland, **1994**.
[27] M. Stebler-Röthlisberger, W. Hummel, P.-A. Pittet, H.-B. Bürgi, A. Ludi, A. E. Merbach, *Inorg. Chem.* **1988**, *27*, 1358–1363.
[28] R. M. Cornell, U. Schwertmann in *The Iron Oxides: Structure, Properties, Reactions, Occurences and Uses*, Wiley-VCH, Weinheim, **1996**.
[29] a) F.-A. Khan, A. Vallat, G. Süss-Fink, *Catal. Commun.* **2011**, *12*, 1428–1431; b) A. Meister, G. Meister, G. Süss-Fink, *J. Mol. Catal.* **1994**, *92*, L123–L126; c) G. Süss-Fink, B. Mollwitz, B. Therrien, M. Dadras, G. Laurenczy, A. Meister, G. Meister, *J. Cluster Sci.* **2007**, *18*, 87–95; d) G. Süss-Fink, F.-A. Khan, J. Boudon, V. Spassov, *J. Cluster Sci.* **2009**, *20*, 341–353.
[30] M. D. Abramoff, P. J. Magelhaes, S. J. Ram, *Biophotonics Int.* **2004**, *11*, 36–42.
[31] a) M. Kotani, T. Koike, K. Yamaguchi, N. Mizuno, *Green Chem.* **2006**, *8*, 735–741; b) M. A. Vergés, R. Costo, A. G. Roca, J. F. Marco, G. F. Goya, C. J. Serna, M. P. Morales, *J. Phys. D* **2008**, *41*, 134003–134013.
[32] a) H. P. Klug, L. E. Alexander, *X-ray Diffraction Procedures*, 2nd ed., John Wiley & Sons Inc., **1974**, pp. 687–703; b) A. Patterson, *Phys. Rev.* **1939**, *56*, 978–982.